

Title	Thin-film-integrated power inductor on Si and its performance in an 8-MHz buck converter
Authors	Wang, Ningning;O'Donnell, Terence;Meere, Ronan;Rhen, Fernando M. F.;Ó Mathúna, S. Cian;Roy, Saibal
Publication date	2008-11
Original Citation	Wang, N., O'Donnell, T., Meere, R., Rhen, F.M.F., Roy, S., Ó Mathúna, S.C., 2008. Thin-film-integrated power inductor on Si and its performance in an 8-MHz buck converter. IEEE Transactions on Magnetics, 44(11), pp. 4096-4099
Type of publication	Article (peer-reviewed)
Link to publisher's version	<a href="http://ieeexplore.ieee.org/stamp/stamp.jsp?arnumber=4717618&amp;isnumber=4717307">http://ieeexplore.ieee.org/stamp/stamp.jsp?arnumber=4717618&amp;isnumber=4717307</a> - 10.1109/TMAG.2008.2001584
Rights	© 2008 IEEE. Personal use of this material is permitted. However, permission to reprint/republish this material for advertising or promotional purposes or for creating new collective works for resale or redistribution to servers or lists, or to reuse any copyrighted component of this work in other works must be obtained from the IEEE
Download date	2024-05-07 01:36:04
Item downloaded from	<a href="https://hdl.handle.net/10468/46">https://hdl.handle.net/10468/46</a>



# UCC

**University College Cork, Ireland**  
Coláiste na hOllscoile Corcaigh

# Thin-Film-Integrated Power Inductor on Si and Its Performance in an 8-MHz Buck Converter

Ningning Wang, Terence O'Donnell, Ronan Meere, Fernando M. F. Rhen, Saibal Roy, and S. Cian O'Mathuna

Microsystems Centre, Tyndall National Institute, Lee Maltings, Cork, Ireland

**This paper presents a microinductor fabricated on silicon using electrochemical techniques that has high efficiency in a low power dc–dc converter. Small signal measurements show a flat frequency response up to 20 MHz with a self resonant frequency of 130 MHz. The inductance at low frequency is approximately 440 nH with a dc resistance of 0.5  $\Omega$ , and a high quality factor of 11.7 at 5.5 MHz. The current handling capability test shows less than 10% decrease in inductance at 500-mA current. The performance of the microinductor has been compared to a conventional chip inductor in a commercially available 8-MHz buck converter. The converter maximum efficiency when using the microinductor is shown to be approximately 3% lower than the one using the conventional discrete chip inductor. However, the profile of the microinductor is much lower than that of the discrete chip inductor. The maximum efficiency of the microinductor in the converter is estimated to be approximately 92%.**

*Index Terms*—dc–dc power conversion, monolithic integrated circuits, thin film inductors.

## I. INTRODUCTION

**T**HERE is an ever increasing demand to miniaturize the voltage regulators that are finding increased use in portable electronic devices. Although there has been considerable recent progress in the integration of the active parts of such converters, significant miniaturization of the overall converter is retarded by the need to miniaturize and integrate the passive components [1]–[13]. Recently, research activities within several major semiconductor companies have suggested that the operating frequency of converters may be increased to as high as several hundred megahertz [14]–[16]. At such high frequencies, the values of inductance required are small, which would allow significant reduction of the overall size of the converter. Commercial products also have reflected the trend with the operating frequency pushed up to 8 MHz [17]. The relatively small inductance value required at this frequency has allowed integration of the inductor into the package [17], [18] side by side with the converter integrated circuit (IC). The technology developed by the authors is aimed at seeking further size reduction by facilitating integration of inductors on to silicon, thus potentially allowing for a stacked approach to the inductor and IC. This provides monolithic power-supply-on-chip (PSOC) solutions with an adequate performance for low-power consumption applications in the portable electronic devices, such as personal digital assistants (PDAs), and mobile phones [19].

Sputtering and electroplating are widely used to deposit the magnetic materials for the magnetic core in microinductors. Sputter deposited magnetic materials can generally have high resistivity, which results in low core eddy current loss and a relatively high  $Q$  factor of the microinductor [3]–[8]. Several reported works have demonstrated such microinductors in dc–dc converters switching at frequencies between 1.2 and 5 MHz with achieved converter efficiencies mostly around 80%.

Notably, the work of Nakazawa *et al.* [7] has even demonstrated the direct integration of a microinductor on top of an active circuit, which made use of a 9- $\mu\text{m}$ -thick sputtered deposited magnetic core. However, sputter deposition may not be the most cost-effective approach for the deposition of relatively thick layers (several microns). Electroplating is generally considered to be a more cost-effective approach for the deposition of thick layers. The works of several researchers have demonstrated microinductors fabricated using electroplated cores [9]–[13]. However, the electroplated materials generally have low resistivity, which leads to high eddy current loss and relatively low  $Q$  factor. Among the microinductors with an electroplated magnetic core, only one inductor has been demonstrated in a dc–dc converter. Although it uses a laminated core, the highest efficiency achieved is 75% [11].

Electroplating is chosen as the core deposition method in this work because it is not only an inexpensive and faster approach for depositing thick layers compared to other techniques but it also readily lends itself to the complex 3-D topology giving a closed magnetic core. The magnetic material used is Ni<sub>45</sub>Fe<sub>55</sub> alloy, which has a resistivity of 45  $\mu\Omega\cdot\text{cm}$ . The fabricated device shows a high  $Q$  factor, and a high efficiency, comparable to those of the reported inductors using sputtered materials. The technology for the device design, fabrication, and the device electrical performance will be introduced in Section II. In previous work [20], the authors presented the predicted performance of a microfabricated inductor in a 4-MHz converter. In this work, a microinductor has been specially designed and optimized for operation at 10 MHz, and tested with a commercially available 8-MHz buck converter. This work also compares the performance of the microinductor to that of a commercially available chip inductor. This is important in that ultimately the relative performance of the microinductor compared to the discrete chip inductor will be one of the most important factors in determining whether microinductors are practical for use in low-power dc–dc conversion. The performance and the loss analysis of both inductors are given in Section III. Conclusions and future development will be given in Section IV.

Digital Object Identifier 10.1109/TMAG.2008.2001584

Color versions of one or more of the figures in this paper are available online at <http://ieeexplore.ieee.org>.

TABLE I  
SPECIFICATIONS OF CONVERTER AND INDUCTOR

Converter Specifications	Values
Input Voltage, V	3.6
Output Voltage, V	1.2
Operating Frequency, MHz	10
Load Current, A	0.5
Ripple Current Ratio,	0.4
Inductor Specifications	Values
Number of turns	7
Winding width, $\mu\text{m}$	50
Spacing, $\mu\text{m}$	50
Winding thickness, $\mu\text{m}$	50
Core length, mm	3.85
Core thickness, $\mu\text{m}$	4.2
Device length, mm	5.76
Device width, mm	2.0

## II. DEVICE DESIGN AND FABRICATION

In previous work, the authors have developed an analytical model for thin film microinductors [20]. The model consists of a winding model, core eddy current model, and core hysteresis model. It can accurately predict the inductance, winding resistance, and hence the various losses within an inductor, such as winding loss, core hysteresis loss, and core eddy current loss. The model has been validated by both finite element analysis and experiment results, and is used in inductor design and optimization. Given the converter specifications, an optimization program based on the inductor analytical model can automatically seek the most efficient inductor design and determine the geometrical parameters of the inductor. Using this optimization program, an inductor was designed for use in a 10-MHz buck converter. The specifications of the converter and inductor are shown in Table I.

The details of the device fabrication process have been described in [20]. The fabricated inductor consists of a single layer of race track shaped copper winding (seven turns) sandwiched between two layers of magnetic material (NiFe alloy) deposited by electroplating. A top view of the fabricated device is shown in Fig. 1.

The frequency characteristic of the inductor has been measured using a Vector Network Analyzer, Model ZRVE (R&S, Germany). The device inductance and resistance were measured at a frequency up to 1 GHz. The measured inductance, resistance, and the quality factor of the device are shown in Fig. 2. The modeled inductance and resistance are also shown in Fig. 2, which match quite well with the measured ones at low frequencies. The discrepancies at high frequency are due to the parasitic capacitance, which is not included in the analytical model. However, the impact of the parasitic capacitance on device performance at low frequency is negligible. It can be seen from the graph that the device has a very flat frequency response and the inductance holds up to at least 20 MHz. The resistance of the inductors increases rapidly for frequencies above 20 MHz and this increase is largely due to eddy current loss in the core. The self-resonant frequency (SRF) of the inductor is 130 MHz.

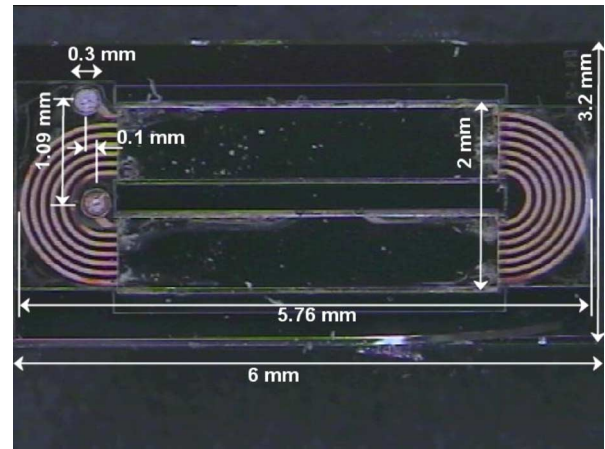


Fig. 1. Top view of the fabricated microinductor.

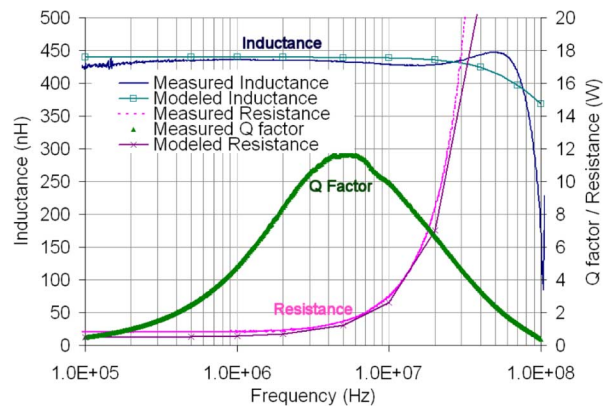


Fig. 2. Measured inductance, resistance, and quality factor.

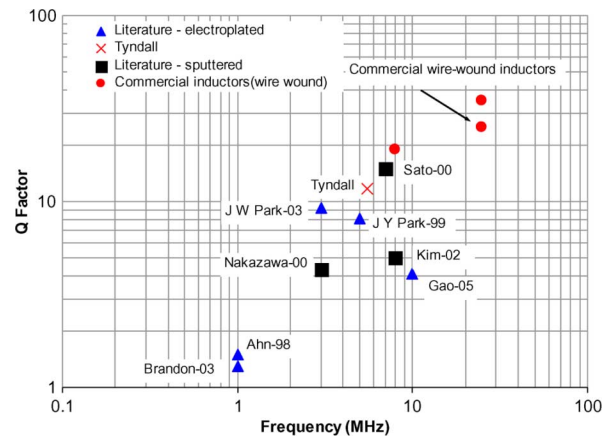


Fig. 3. Quality factors of microinductors fabricated using standard IC fabrication compatible process.

The measured inductance at low frequency is approximately  $0.44 \mu\text{H}$  and the measured dc resistance is  $0.5 \Omega$ .

The  $Q$  factor of the microinductor in this work has been compared to those microfabricated inductors from the literature either using electroplating or sputtering deposition technique for the magnetic core, as shown in Fig. 3. The graph shows that the fabricated inductor in this work has achieved a  $Q$  factor of 11.7 at 5.5 MHz. This is the highest  $Q$  factor among those reported microinductors fabricated using electroplating techniques, and

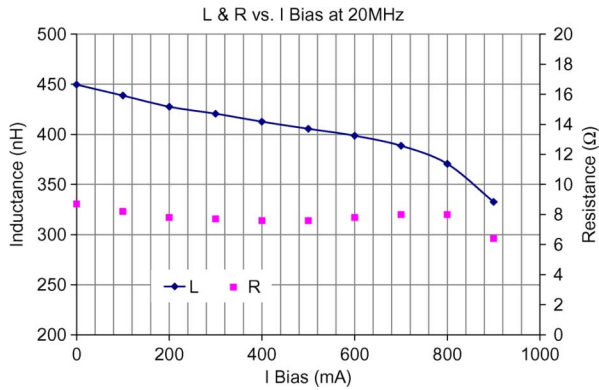


Fig. 4. Measured inductance at 20 MHz versus dc bias current.

higher than that achieved using a laminated core [11], [12]. It is also comparable to the  $Q$  factor of the microinductor using sputtered magnetic materials. For example, the microinductor reported by Sato *et al.* [3], which had  $Q$  factor of 15, used a core material of FeCoBN that had a resistivity of  $3000 \mu\Omega\cdot\text{cm}$ .

In addition to the small signal frequency characteristic, the characteristic under dc bias current is also a very important parameter when evaluating a power inductor. The current carrying capability of the microinductor has been measured at 20 MHz using an HP LCR Meter 4285 A with an HP current source 42841 A. The test results are shown in Fig. 4.

The bias current characteristic test shows that the inductance only drops by approximately 10% with a 500-mA dc current, which implies that it is capable of handling at least 500-mA current without saturation. In fact, the measurement shows that full core saturation occurs for currents greater than 800 mA. There is no significant change of the resistance, which indicates that the core loss remains the same while the dc bias current is increased.

### III. PERFORMANCE IN AN 8-MHz BUCK CONVERTER

The microinductor has also been tested in a buck converter. The MIC2285 is a commercially available buck converter with a fixed switching frequency of 8 MHz from Micrel, USA [21]. This represents the highest switching frequency buck converter presently available on the market. It requires a  $0.47\text{-}\mu\text{H}$  external inductor and operates from a 2.7- to 5.5-V input with an output current up to 500 mA. The MIC2285YML is the corresponding evaluation board available from the same company. Its output voltage is fixed to 1.8 V. The evaluation board is used in the electrical performance test of the microinductor. An inductor from Murata, Japan (part number LQM21PNR47M00) with an inductance of  $0.47 \mu\text{H}$  was originally mounted on the evaluation board. This chip inductor uses a 0805 standard chip size ( $2 \text{ mm} \times 1.25 \text{ mm}$ ) and is 0.55 mm thick. It has a dc resistance of  $0.12\Omega$ , which to the authors' knowledge is one of the lowest dc resistance  $0.47\text{-}\mu\text{H}$  inductors with the thinnest profile available in a 0805 package. The converter efficiency was first measured using this inductor and then the microfabricated thin film inductor was used to replace the chip inductor. A picture of the converter evaluation board with microinductor wire bonded on top is shown in Fig. 5. The measured efficiencies of the buck converter using the on silicon integrated thin film inductor with

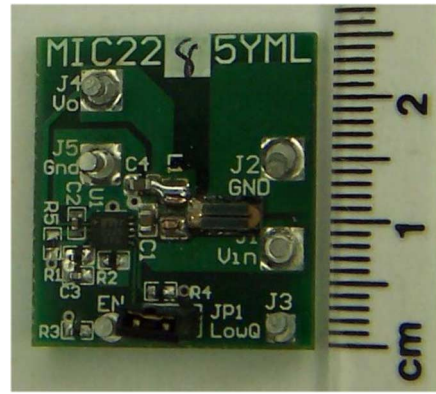


Fig. 5. Tyndall microinductor mounted on an 8-MHz commercially available buck converter evaluation board.

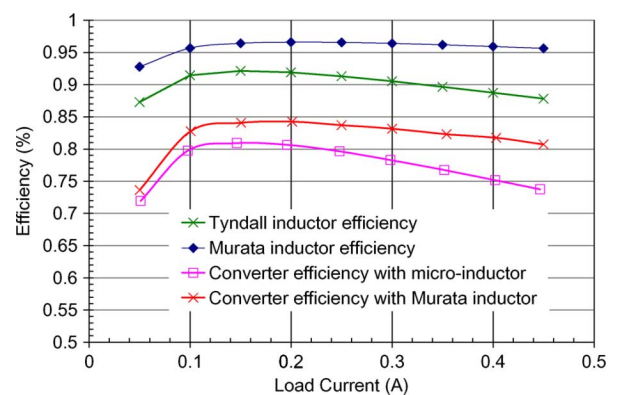


Fig. 6. Measured converter efficiencies and estimated inductors efficiencies.

various load currents are shown in Fig. 6. In the efficiency measurements, the input voltage of the converter is 3.6 V and the output voltage is fixed to 1.8 V. The load current varies from 50 to 450 mA. The efficiencies of the converter using the original chip inductor are also shown in the graph for comparison.

The difference in converter maximum efficiency between using the commercially available chip inductor and microinductor is approximately 3%. When using the microinductor, the converter efficiency is still over 80% for the load current between 0.1 and 0.25 A.

Using the aforementioned analytical models developed for the microinductor, the measured frequency characteristic of the chip inductor provided by Murata, the inductor efficiency in this converter can be estimated. These inductor efficiency curves are also included in Fig. 6. The inductor efficiency curves are consistent with the measured converter efficiency, in that the efficiency of the microinductor is shown to be approximately 3% lower than that of the wire-wound inductor. The peak microinductor efficiency is approximately 92%. To further illustrate the reason for the difference in efficiency between the inductors, the graph in Fig. 7 shows the breakdown of losses in the inductors as obtained from the models. The loss has been separated into ac loss and dc loss. Due to the nature of the chip inductor impedance model (S parameters) provided by Murata, it is not possible to further separate the ac loss into core loss and winding loss. The dc loss of the chip inductor is calculated using the dc resistance and the dc component of the load current. The ac loss

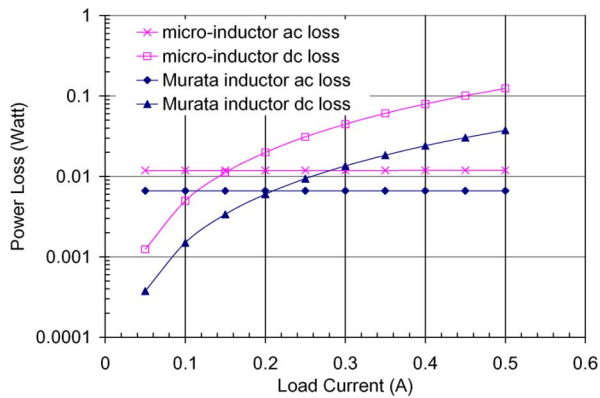


Fig. 7. The ac and dc loss for the microinductor and the chip inductor.

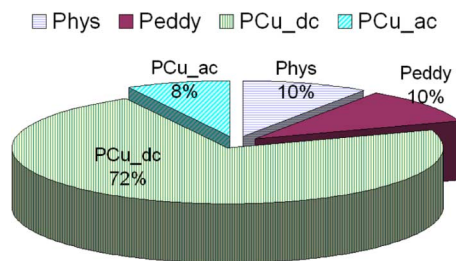


Fig. 8. Breakdown of losses in the microinductor for 250-mA dc current.

is the sum of the losses at each harmonic, given current and impedance at each harmonic frequency. The loss breakdown shows that the wire-wound inductor has lower ac loss and lower dc loss. The ac loss dominates in both inductors at low current levels as expected. For the microinductor dc loss exceeds ac loss at higher current levels.

For the microinductor, the loss can also be examined in terms of the split between winding loss (both ac and dc) and core loss. The diagram in Fig. 8 shows the breakdown of losses in the microinductor for a load current of 250 mA. This shows that the winding loss is substantially dc conduction loss and the dc conduction loss contributes 72% of the total inductor loss. The eddy current loss and hysteresis loss in the core contribute 20% of the total inductor loss.

#### IV. CONCLUSION

This work demonstrated the feasibility of implementing thin film microinductors in a dc–dc converter. The loss distribution within the microinductor has been investigated and compared to that of a chip inductor. The analysis has shown that the microinductor has a peak efficiency of approximately 92% and is 3% less efficient than a conventional chip inductor. This is mainly due to substantial winding dc conduction loss. The dc resistance of the microinductor can be reduced either by increasing the conductor thickness or using a laminated core. Currently, the copper conductor thickness is 50  $\mu\text{m}$ . It may be possible to increase the conductor thickness to more than 80  $\mu\text{m}$ . Addition-

ally, by using a laminated core, a smaller number of turns can be used to give the same inductance but with smaller dc resistance without increasing the core eddy current loss. The core lamination process has been demonstrated previously in micro-transformer fabrication [22].

The thin film inductor has a relatively large footprint area ( $2 \times 5.76 \text{ mm}^2$ ) compared to that of the chip inductor ( $2 \times 1.25 \text{ mm}^2$ ). It is very difficult to compete with the chip inductors in terms of inductance per unit area, because the chip inductors have a thicker profile, and hence use a considerably larger volume of Ferrite material. The chip inductor tested in this work is 0.55 mm thick, whereas the effective part of the microinductor is less than 0.15 mm. The greatest size reduction in a converter can be achieved by the stacking of the passive and active components in which case the very low profile can be a great advantage for microinductors. Moreover, the IC fabrication compatible process developed by authors allows fabricating inductors onto the same substrate or even directly on top of the power management IC to realize a truly monolithic dc–dc converter without the requirement of postprocessing packaging.

#### ACKNOWLEDGMENT

This work was supported by Enterprise Ireland (EI) under the Industry Led Research Program in Power Electronics.

#### REFERENCES

- [1] Y. Fukuda *et al.*, *IEEE Trans. Magn.*, vol. 39, p. 2057, Jul. 2003.
- [2] M. Yamaguchi *et al.*, *IEEE Trans. Magn.*, vol. 31, no. 6, p. 4229, 1995.
- [3] T. Sato *et al.*, in *Proc. Int. Power Electron. Conf.*, Tokyo, Japan, 2000, p. 303.
- [4] Y. Sasaki *et al.*, in *Proc. Int. Power Electron. Conf.*, Tokyo, Japan, 2000, p. 315.
- [5] C. S. Kim *et al.*, *IEEE Trans. Magn.*, vol. 37, no. 4, p. 2894, 2001.
- [6] K. H. Kim *et al.*, *IEEE Trans. Magn.*, vol. 38, no. 5, p. 3162, 2002.
- [7] H. Nakazawa *et al.*, *IEEE Trans. Magn.*, vol. 36, no. 5, p. 3518, 2000.
- [8] S. Prabhakaran *et al.*, in *Proc. IEEE 36th Power Electron. Specialists Conf.*, 2005, p. 1513.
- [9] E. J. Brandon *et al.*, *IEEE Trans. Magn.*, vol. 39, p. 2049, 2003.
- [10] C. H. Ahn *et al.*, *IEEE Trans. Ind. Electron.*, vol. 45, p. 866, 1998.
- [11] J. W. Park *et al.*, *IEEE Trans. Magn.*, vol. 39, no. 5, p. 3184, 2003.
- [12] J. Y. Park *et al.*, *IEEE Trans. Magn.*, vol. 35, no. 5, p. 4291, 1999.
- [13] X. Gao *et al.*, *IEEE Trans. Magn.*, vol. 41, no. 12, p. 4397, 2005.
- [14] G. Schrom *et al.*, in *Proc. IEEE 22nd Annu. Appl. Power Electron. Conf.*, Feb. 2007, p. 727.
- [15] V. Pinon *et al.*, in *Proc. 18th Int. Symp. Power Semiconductor Devices IC's*, Naples, Italy, Jun. 4–8, 2006, p. 1.
- [16] G. Schrom *et al.*, in *Proc. 35th Annu. IEEE Power Electron. Specialists Conf.*, Aachen, Germany, 2004, p. 4702.
- [17] Micrel, MIC3385 [Online]. Available: [http://www.micrel.com/\\_PDF/mic3385.pdf](http://www.micrel.com/_PDF/mic3385.pdf)
- [18] EN5312Q, Enpirion [Online]. Available: <http://www.enpirion.com/pdfdocuments/EN5312Q%20Rev%2011.pdf>
- [19] S. C. O'Mathuna *et al.*, *IEEE Trans. Power Electron.*, vol. 20, no. 3, p. 585, 2005.
- [20] N. Wang *et al.*, *J. Magn. Magn. Mater.*, vol. 316, p. e233, 2007.
- [21] Micrel, MIC2285YML [Online]. Available: [http://www.micrel.com/\\_PDF/mic2285.pdf](http://www.micrel.com/_PDF/mic2285.pdf)
- [22] M. Brunet *et al.*, *J. Microelectromech. Syst.*, vol. 15, no. 1, p. 94, Feb. 2006.

Manuscript received March 03, 2008. Current version published December 17, 2008. Corresponding author: N. Wang (e-mail: ning.wang@tyndall.ie).